

Paleogene Tectonic Evolution Controls on Sequence Stratigraphic Patterns in the Fushan Sag, Northern South China Sea

Guanhong Wang^{*1,2}, Hua Wang¹, Huajun Gan¹, Entao Liu^{2,3}, Cunyin Xia⁴,
Yingdong Zhao², Shanbin Chen², Chengcheng Zhang²

1. Key Laboratory of Tectonics and Petroleum Resources of Ministry of Education, China University of Geosciences, Wuhan 430074, China

2. Faculty of Earth Resources, China University of Geosciences, Wuhan 430074, China

3. School of Earth Sciences, The University of Queensland, Brisbane QLD 4072, Australia

4. Exploration and Development Corporation, PetroChina, Guangzhou 510240, China

ABSTRACT: Tectonism is of extreme importance to sequence stratigraphic patterns in continental sedimentary basins, affecting both the architectures and internal makeup of sequences. Sequence stratigraphic framework of the Paleogene system in the Fushan sag, northern South China Sea, was built using 3D and 2D seismic data, complemented by drilling cores and well logs data. One first-order, three second-order and seven third-order sequences were identified. Analysis of paleotectonic stress field, unconformities and subsidence history showed that the Paleogene tectonic evolution presented significant characteristics of multistage and episode, and can be divided into three stages: rifting stage I (initial rifting period), rifting stage II (rapid subsidence period), rifting stage III (fault-depressed diversionary period). Partition of the west and east in tectonic activity was obvious. The west area showed relatively stronger tectonic activity than the east area, especially during the rifting stage II. Episodic rifting and lateral variations in tectonic activity resulted in a wide variety of structural slope break belts, which controlled both the sequence architectures and interval makeup, and strongly constrained the development of special facies zones or sand bodies that tended to form hydrocarbon accumulation. This paper classifies the genetic types of slope break belts and their relevant sequence stratigraphic patterns within the Fushan sag, and further discusses the tectonic evolution controls on sequence stratigraphic patterns, which suggests that vertical evolution paths of structural slope break belts and relevant sequence stratigraphic patterns as a response to the Paleogene tectonic evolution were strongly controlled by sag margin types and lateral variations of tectonic activity.

KEY WORDS: South China Sea, Fushan sag, tectonic evolution, structural slope break belt, sequence stratigraphic pattern.

0 INTRODUCTION

After several decades, the theory of sequence stratigraphy from the passive continental margin basin has been fully developed (Catuneanu et al., 2009; Xie et al., 2008; van Wagoner et al., 1990; Vail et al., 1977) and widely applied to inland basins, which has not only broadened the oil and gas exploration field, but also enriched the theory of sequence stratigraphy (Huang et al., 2012; Lin, 2009; Li et al., 2002; Xu, 1997). With further research, it has been realized that architectures and internal makeup of sequences have extremely close genetic connection with tectonism in continental rift basins. Especially

in recent years, the tectono-sequence stratigraphy has become a major international theme of sedimentary basin analysis, and plays a vital role in establishing sequence stratigraphic patterns and predicting favorable reservoirs (Song et al., 2014; Huang et al., 2012; Feng et al., 2010; Lin et al., 2001).

With an increasing demand on petroleum resources in China, the Fushan sag has recently become a focal point for intensive petroleum exploration within old fields. A quantity of new data from PetroChina, including high-quality seismic data covering the whole sag, well logs and drilling cores, provide an excellent basis for the tectono-sequence stratigraphy analysis. Based on the analyses of tectonic evolution history, sag margin types, fault combination patterns and sedimentary facies, this paper classifies the genetic types of structural slope break belts and summarizes sequence stratigraphic patterns within the Fushan sag, which not only enhances the understanding of tectonic evolution controls on sequence stratigraphic patterns, but also offers scientific evidence for predicting favorable explora-

*Corresponding author: wangguanhong2015@163.com

© China University of Geosciences and Springer-Verlag Berlin Heidelberg 2016

Manuscript received November 7, 2014.

Manuscript accepted August 22, 2015.

tion zones in particular tectonic positions under sequence stratigraphic framework.

1 REGIONAL GEOLOGICAL SETTING

The Fushan sag, located in the southeast of the Beibuwan Basin, northern South China Sea, was formed in extensional environment during Cenozoic, with a total area of approximately 2 920 km² (Shi et al., 2007). It is bounded to the west by the Lingao fault, to the south by the Anding fault, and to the east by the Changliu fault (Fig. 1). Controlled by asymmetric stretching setting resulting from sinistral strike slip of the Red River fault zone and clockwise rotation of the Hainan uplift

(Wang et al., 2014), a transfer zone was developed in the central region and divided the whole sag into two sub-sags (the Huangtong sub-sag in the west and the Bailian sub-sag in the east), resulting in different tectonic styles and sedimentary patterns between the west and east areas (Liu et al., 2012).

During Paleogene, the depositional environment changed from lake in the early period through fluvial facies to costal plain in the late period. The synrift basin fills of the Cenozoic system are about 3 000–5 000 m thick and comprise, in ascending order, the Paleogene Changliu, Liushagang and Weizhou formations, and the Neogene Xiayang, Jiaowei, Dengloujiao and Wanglougang formations (Fig. 2).

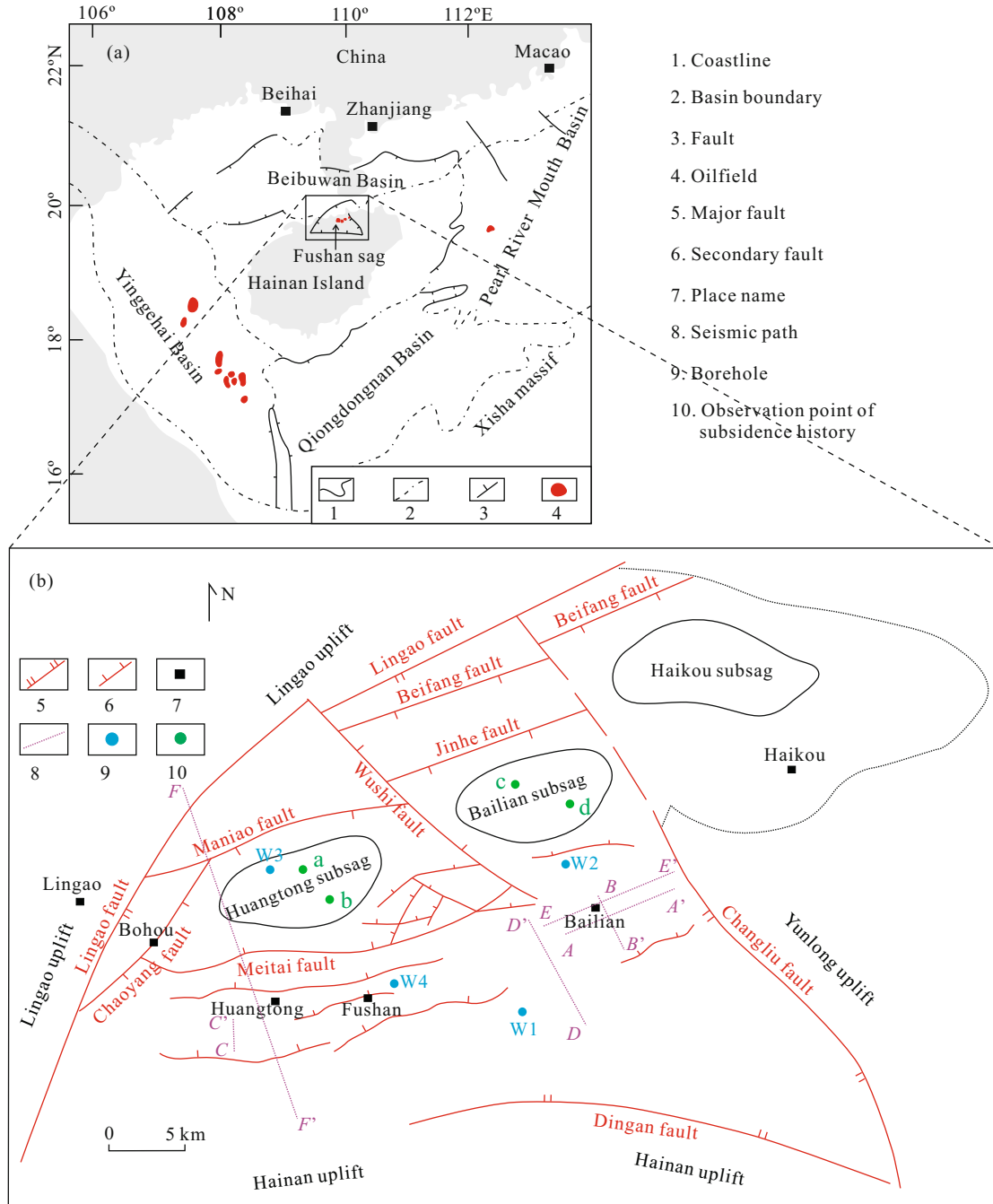


Figure 1. (a) Map showing the sedimentary basins in the northern margin of the South China Sea and the location of the Fushan sag, the box indicates the area shown in (b); (b) the Fushan sag and its structural units division.

In the Fushan sag, the clastic sediments were mainly supplied by the Hainan uplift, followed by the Lingao and Yunlong uplifts (Liu et al., 2014). Large-scale faults mainly included the NE-trending Lingao fault and its adjustment faults (Chaoyang fault, Maniao fault, Beifang fault and Jinhe fault), the NW-trending Changliu fault and the NEE-trending Meitai fault (Fig. 1).

2 MATERIALS AND METHODS

Data sets in this study consist of 3D seismic data cube, 2D seismic profiles, well logs data and some drilling cores data. The 3D seismic data cube comprises a region of approximately 2 000 km², covering the major hydrocarbon exploration area. The peak frequency is about 35 Hz. In addition, several 2D seismic profiles have been carried out in the northern sag where the 3D seismic data have not covered.

In this paper, we use high-quality seismic data, well logs and latest geological documents as the basic data to construct the sequence stratigraphic framework. The sequence classification developed by Vail et al. (1977) is proposed for the Fushan sag. Within the sequence stratigraphic framework, through stress field analysis, unconformities analysis and backstripping

procedure, the quantitative study of tectonic evolution is carried out. In the end, tectonic evolution controls on structural slope break belts and sequence stratigraphic patterns were discussed.

3 SEQUENCE STRATIGRAPHY

Sequence stratigraphy establishes a chronostratigraphic framework bounded by unconformities or their correlative conformities. The recognition of sequence boundaries contributes to building the chronostratigraphic framework. In the Fushan sag, sequence stratigraphic surfaces are identified based on 3D and 2D seismic profiles, complemented by well logs and some cores data. The following criteria are used to recognize sequence boundaries.

(1) In general, unconformities and their correlative conformities are defined as sequence boundaries, for they represent time-barrier surfaces (Haq et al., 1987). Truncations, surfaces of onlap, downlap and toplap are the reflection of unconformable stratigraphic contacts on seismic profiles (Fig. 3a).

(2) Sequence boundaries can also be represented by abrupt changes in physical characteristics such as sedimentary facies and lithology. Abrupt changes of seismic reflection characteristics or log curves can be used to identify such boundaries (Fig. 3b).

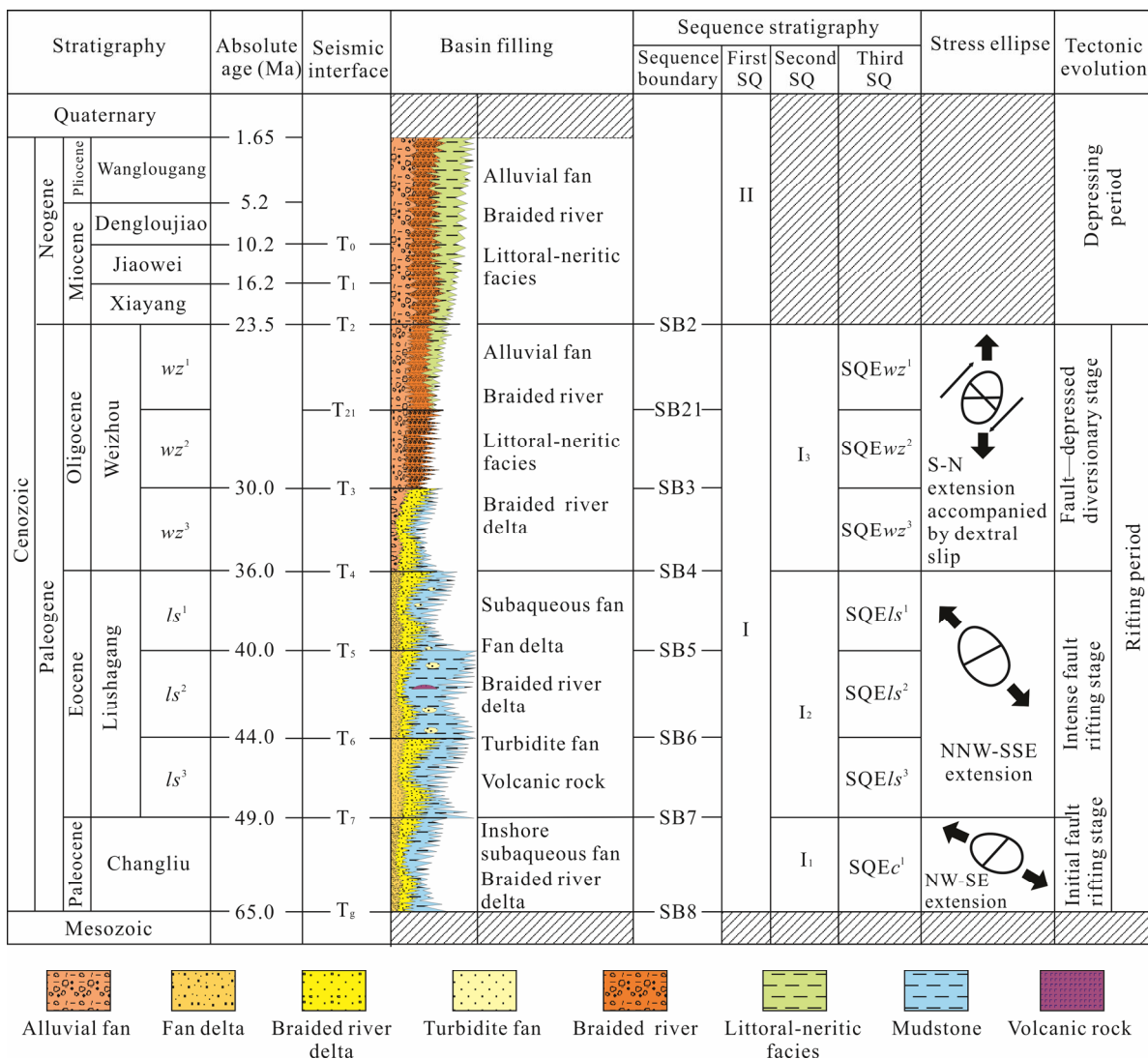


Figure 2. The basin filling evolution and stratigraphic sequence division of the Fushan sag.

Based on preceding criteria, combined with previous sequence stratigraphy study results, three orders of unconformity-bounded sequence are recognized within the Paleogene system of Fushan sag (Figs. 2 and 4). The entire Paleogene system is considered to be a first-order sequence and contains three second-order sequences, which correspond to the Changliu Formation, Liushagang Formation and Weizhou Formation from bottom to top, respectively. The second-order sequences can be subdivided into one or three third-order sequences. The Paleogene system contains seven third-order sequence stratigraphic cycles (SQEc¹, SQEl³, SQEl², SQEl¹, SQEwz³, SQEwz² and SQEwz¹) from bottom to top in total.

4 PALEOGENE TECTONIC CHARACTERISTICS WITHIN THE FUSHAN SAG

4.1 Paleogene Tectonic Evolution within the Fushan Sag

In the Fushan sag, the tectonic evolution is identified mainly based on: (1) change of stress field (Lei et al., 2011); (2)

regional unconformities (Feng et al., 2010); (3) subsidence history (Li et al., 1999).

4.1.1 Analysis of stress field

Tectonic evolution can be implied by the change of stress field (Lei et al., 2011; Xu et al., 2011). In the Fushan sag, SB4 and SB7 are key tectonic evolutionary boundaries (Fig. 2), indicating that the Paleogene tectonic evolution experienced three different stages (Zhang et al., 2013). The NW-SE extensional tectonic stress field resulted in the embryonic form of the Fushan sag, which showed an overall “dustpan” shape controlled by the NE-trending Lingao fault. Subsequently, the NNW-SSE extensional tectonic stress field resulted in the formation of numerous NEE-trending syndepositional secondary faults. The succeeding S-N extension accompanied by dextral slip was much weaker than the preceding NNW-SSE extension. Accordingly, the tectonic activity became weaker and downwarp action became stronger gradually.

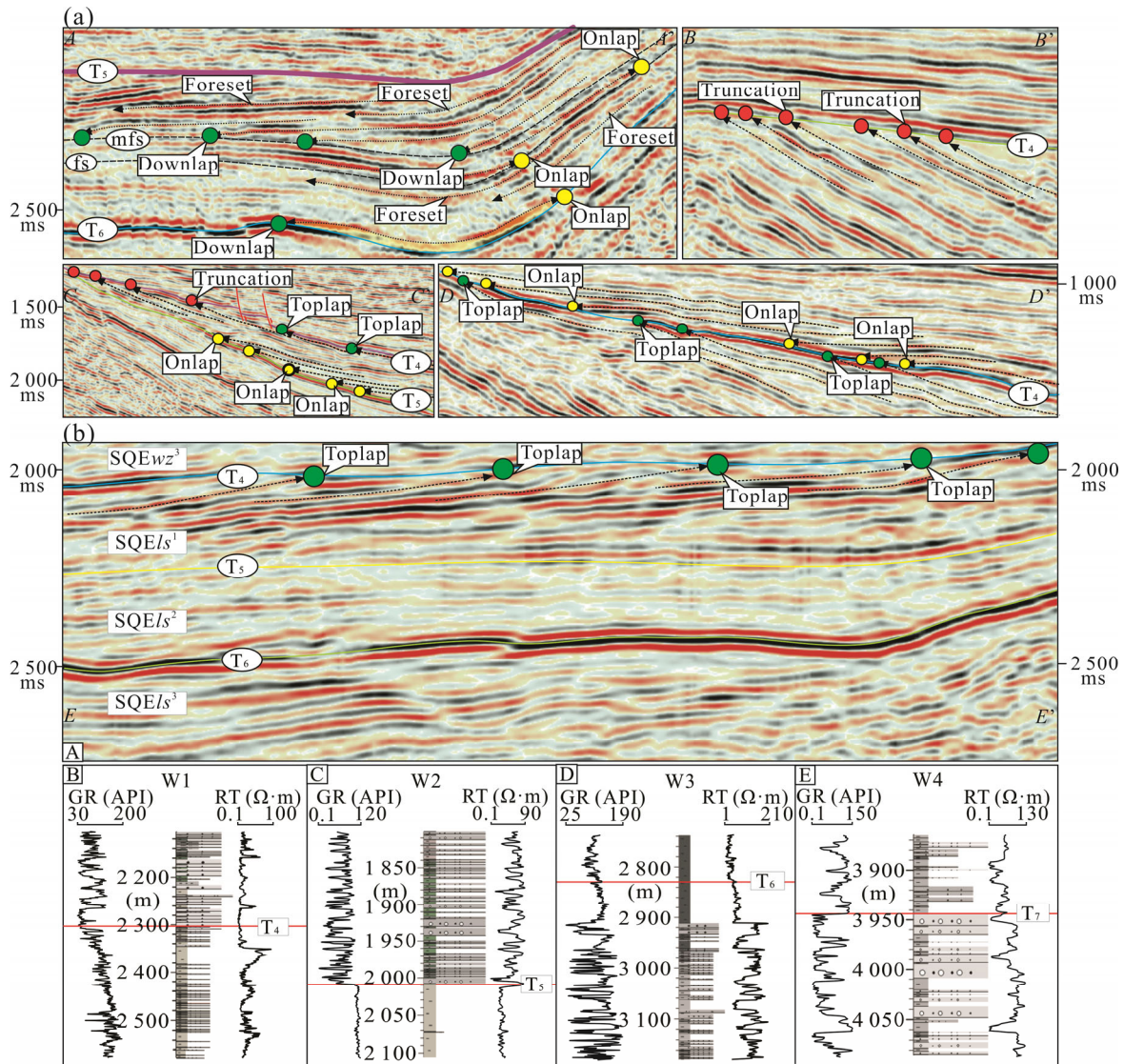


Figure 3. (a) Seismic reflection features of sequence boundaries showing onlap, downlap, toplap and truncation. (b) A. The difference of seismic reflection characteristics up or down boundary SB5 and SB6. The strata between SB5 and SB6 present the characteristics of middle reflection and middle continuity, which is different from the strata up or down. B, C, D, E. Characteristics of unconformities feature abrupt changes in lithology or sedimentary facies in well logs. See Fig. 1 for the locations of seismic profiles and wells.

4.1.2 Analysis of unconformities

It has been suggested that strata unit bounded by unconformities is usually consistent with the episodic and cyclic characteristics of tectonic evolution (Feng et al., 2010; Lin et al., 2001). Based on distribution range and duration of deposition break, unconformities can be classified into three orders. The first-order uniformities, commonly regional unconformities, are generated by significant tectonic movements, representing large-scale truncation and prolonged deposition lacuna. The second-order uniformities are always controlled by uplift following each rifting episode and are related to the change of paleotectonic stress field. The third-order uniformities, local erosional truncations, commonly result from fluctuation of lake level or sediment supply rate (Lin et al., 2001).

Based on the 2D and 3D seismic data and well logs data, combined with previous researches (Ma et al., 2013; Xu et al., 2011), the interpretive scheme of unconformities in the Fushan sag is as follows. (1) The top (SB2) and the bottom (SB8) boundaries of the Paleogene system, corresponding to the first-order sequence boundaries, are defined as first-order unconformities. They are angular unconformities that can be traceable throughout the whole Beibuwan Basin. (2) Two second-order unconformities (SB4, SB7) divide the paleogene system of the Beibuwan Basin into three second-order sequences. They are regional unconformities that extend into the central basin. (3) Four three-order unconformities (SB21, SB3, SB5, and SB6) can be recognized in the Paleogene of the Beibuwan Basin. They are local unconformities that are mainly distributed in the basin margins (Ma et al., 2013). Only the SB5 can be recognized in the Fushan sag.

4.1.3 Analysis of subsidence history

Using the backstripping procedure (Allen and Allen, 2005; Li et al., 2004; Lin et al., 2004), the Paleogene subsidence history of the Fushan sag has been simulated quantitatively. Tectonic subsidence was defined as basin subsidence caused by tectonism. Total subsidence of sedimentary basin relates to tectonism, thermal mechanism, sediment compaction, load and fluctuation of base level. The contribution degree of tectonic subsidence to total subsidence can reflect dominant mechanism of basin subsidence and prototype basin. Figure 5 indicates that the subsidence rate presented significant feature of multistage and episode. According to the total subsidence, tectonic subsidence and their relative changes on subsidence rate, the conclusion has been reached that the tectonic subsidence made less and less contribution to total subsidence with time going by, especially in the late periods of the rifting stage.

4.1.4 Tectonic evolution

The analysis of paleotectonic stress field, unconformities and subsidence history shows that the Paleogene tectonic activity of the Fushan sag underwent Paleogene rifting period (65–23.5 Ma) and Neogene depressing period (23.5 Ma to now). The Paleogene rifting period can be subdivided into three stage: rifting stage I (65–49 Ma), rifting stage II (49–36 Ma) and rifting stage III (36–23.5 Ma).

The rifting stage I was initial rifting period when mainly Changliu Formation was deposited. The tectonic subsidence

rate, maximally 40 m/Ma, accounted for 2/3–3/4 of the total subsidence rate (Fig. 5), indicating that fault controlling action was the dominant mechanism. During this period, the basin filling was characterized by a set of nearshore subaqueous fans along the northern escarpment margin, fan deltas along the eastern escarpment margin and braided river deltas along the ramp margin (Liu et al., 2003).

The rifting stage II was a rapid subsidence period when Liushagang Formation was deposited. During this period, the subsidence rate increased (Fig. 5) and the fault activity became much stronger (Fig. 6). The tectonic subsidence rate, maximally 180 m/Ma, accounted for 1/2–3/5 of the total subsidence rate, indicating that fault controlling action was still the dominant mechanism. Because of the rapid subsidence, the accommodation increased intensively, resulting in the deposition of thick-bedded mudstones. The main types of sand bodies included fan deltas and nearshore subaqueous fans along the escarpment margins, and braided river deltas along the ramp margin (Liu et al., 2003).

The rifting stage III was a fault-depressed diversionary period when Weizhou Formation was deposited. During this period, the subsidence rate decreased remarkably (Fig. 5) and the fault activity became significantly weakened (Fig. 6). The tectonic subsidence rate, maximally 70 m/Ma, accounted for 1/3–1/2 of the total subsidence rate, indicating that faults controlling action had been replaced by interaction of both territorial downwarp actions and fault controlling action. The sag evolved into a flatter terrain and shallower water. Deltaic depositional facies were drawn back, and braided rivers developed widely (Liu et al., 2003).

4.2 Spatial Differences of Tectonic Activity within the Fushan Sag

Asymmetric stretching setting resulted from sinistral strike slip of the Red River fault zone and clockwise rotation of the Hainan uplift, have resulted in different tectonic activities and structural styles between the west and east areas. Accordingly, a transfer zone was developed in the central region to conserve regional extension or extensional strain (Liu et al., 2012).

The Lingao fault limited the western and northern boundaries and dominated the basic shape of the Fushan sag, bounded by the Wushi fault (Fig. 6), the east part of the Lingao fault had relatively weaker activity than the west. The Changliu fault, forming the eastern boundary, had both extension and strike-slip characteristics. Figure 6 shows that the Changliu fault presented lower activity rate than the Lingao fault. In addition, partition of the east and west in subsidence rate was evident as well. Typical observation points (Fig. 5) indicate that the subsidence rate in the east area of the Fushan sag was lower than that of the west area, especially in the rapid subsidence period. These evidences collectively suggest that the Fushan sag was featured by obvious partition of the west and east in Paleogene tectonic activity. The west area showed stronger tectonic activity than the east, especially during the rifting stage II.

5 SEQUENCE STRATIGRAPHIC PATTERNS WITHIN THE FUSHAN SAG

Within the sequence stratigraphy framework, the term

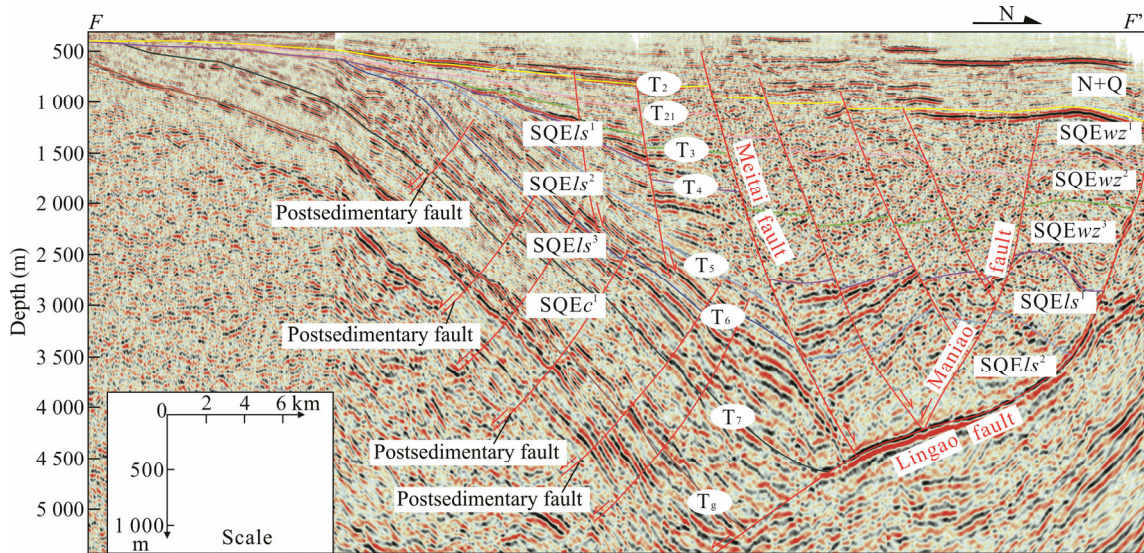


Figure 4. An N-S structural and sequence stratigraphic section across the whole Fushan sag. See Fig. 1 for the location.

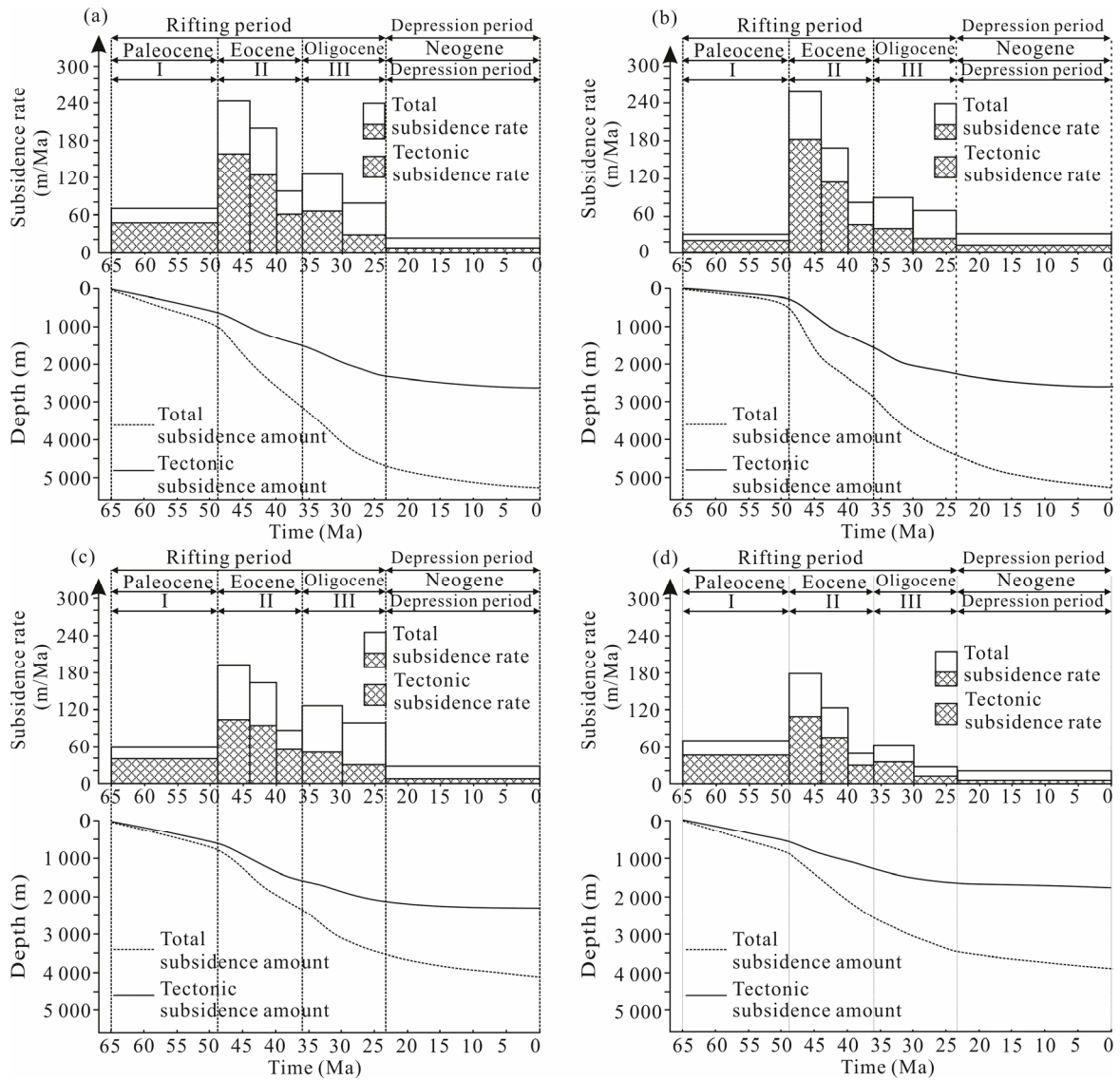


Figure 5. Backstripping total subsidence rate and tectonic subsidence rate of the Fushan sag. See the locations of observation points on Fig. 1.

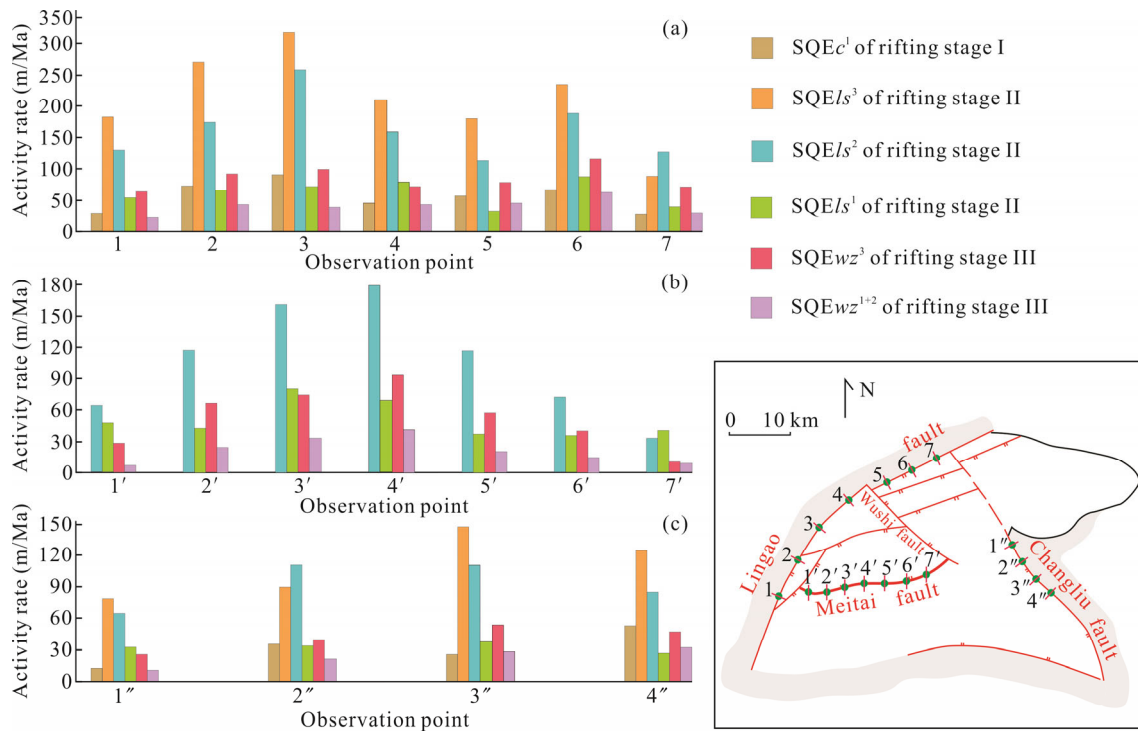


Figure 6. Fault activity of different tectonic evolution stages in the Fushan sag. (a) Activity rate of the Lingao fault; (b) the Meitai fault; and (c) the Changliu fault.

“structural slope break belt” is an important geomorphologic concept which refers to the zone where the gradient suddenly changes. The sudden gradient change is related to syndepositional fracture movement (Liu et al., 2006). Structural slope break belts constrain the changes in accommodation space, mark boundaries between different paleogeomorphic units and sedimentary facies, and play an extremely important role in controlling the internal composition of stratigraphic sequences (Hou et al., 2012; Huang et al., 2012; Feng and Xu, 2006; Ren et al., 2004). Through episodic rifting and lateral variations of subsidence, a wide variety of structural slope break belts can be formed (Liao et al., 2012; Deng et al., 2008), which further controls different sequence stratigraphic patterns.

In the Fushan sag, four types of structural slope break belts were present: steep slope fault belt, steep slope step-fault belt, multi-level step-fault belt, slope break flexure belt. The first two can be subdivided into different evolutionary types (Fig. 7).

5.1 Steep Slope Fault Belt and Relevant Sequence Stratigraphic Patterns

The steep slope fault belt had a paleogeomorphology characterized by a steep slope that was controlled by boundary faults. In the Fushan sag, the boundary faults along escarpment margins were characterized by large fault displacements and steep planes. According to the differences in foot slope, steep slope fault belts can be further characterized as either up-dip or down-dip foot slope belt.

5.1.1 Up-dip foot slope belt and relevant sequence stratigraphic pattern

During the rifting stage I and initial rifting stage II, when Changliu Formation and the third member of Liushagang For-

mation were deposited, the up-dip foot slope belt was developed along the Lingao fault in the northern escarpment margin. We name the relevant sequence stratigraphic pattern as Type A1 Sequence. The up-dip foot slope belt formed the division between denuded and deposition zones. The upthrown wall was exposed and eroded, with incised valleys forming on the paleo-high. Massive clasts, provided by the Lingao uplift, were quickly deposited near the root of the Lingao fault and formed nearshore subaqueous fans. On the seismic profile, nearshore subaqueous fans show high-amplitude low-continuity seismic reflection configuration. Because of close proximity to the source area, their sediments are characterized by poorly sorted coarse clasts, consisting largely of gravels. Due to the abundant accommodation space in the root of the downthrown wall, the fans were thick. However, the areal extension was generally small. The Type A1 Sequence in the sag was composed of low-stand system tract (LST), expanding system tract (EST) and highstand system tract (HST). Because of the up-dip foot, slump fans of delta fronts were absent from the Type A1 Sequence (Fig. 8).

5.1.2 Down-dip foot slope belt and relevant sequence stratigraphic pattern

The down-dip foot slope belt was mainly developed along the Changliu fault in the eastern escarpment margin. We name the relevant sequence stratigraphic pattern as Type A2 Sequence. The down-dip foot slope belt formed the division between denuded and deposition zones. The upthrown wall was exposed and eroded, with incised valleys forming on the paleo-high. Fan deltas were developed on the downthrown wall of the Lingao fault. Fan-delta fronts have medium-amplitude medium-continuity seismic reflective characteristics, showing

an oblique foreset reflection configuration on the seismic section. The sediments of the delta fronts are mainly poorly sorted pebbly coarse-medium sandstones, shown as Core Wa (1 982.6 m). The sediments of the prodeltas are mainly well sorted fine sandstones, shown as Core Wb (2 530.5 m). In the center of the

lake, basin floor fans in the lowstand system tract (LST) and slip blocks of delta fronts in the highstand system tract (HST) can directly deposited within the deep lake mudstones, and tended to form lithologic traps as lens in the lake center. The log curves of Wc (3 900–3 940 m) show obvious figer-shaped,

Structural slope break belts		Evolutional types	Typical types of reservoir facies	Location	Development time
Steep slope fault belt	Up-dip foot slope belt		Incised valley Nearshore subaqueous fan	Northern escarpment margin	Rifting stage I Early period of rifting stage II
	Down-dip foot slope belt		Incised valley Fan delta Turbidite bodies Basin floor fan	Eastern escarpment margin	Rifting stage I Rifting stage II Rifting stage III
Steep slope step-fault belt	Up-dip foot step-fault belt		Incised valley Fan delta	Northern escarpment margin	Middle-late period of rifting stage II
	Down-dip foot step-fault belt		Incised valley Fan delta Turbidite bodies Basin floor fan	Northern escarpment margin	Rifting stage III
Multi-level step-fault belt			Incised valley Braided delta Turbidite bodies Basin floor fan	Southern ramp margin	Middle-late period of rifting stage II Rifting stage III
Slope break flexure belt			Incised valley Braided delta Turbidite bodies Basin floor fan	Southern ramp margin	Middle-late period of rifting stage II Rifting stage III

Figure 7. Types of structural slope break belts developed in the Fushan sag.

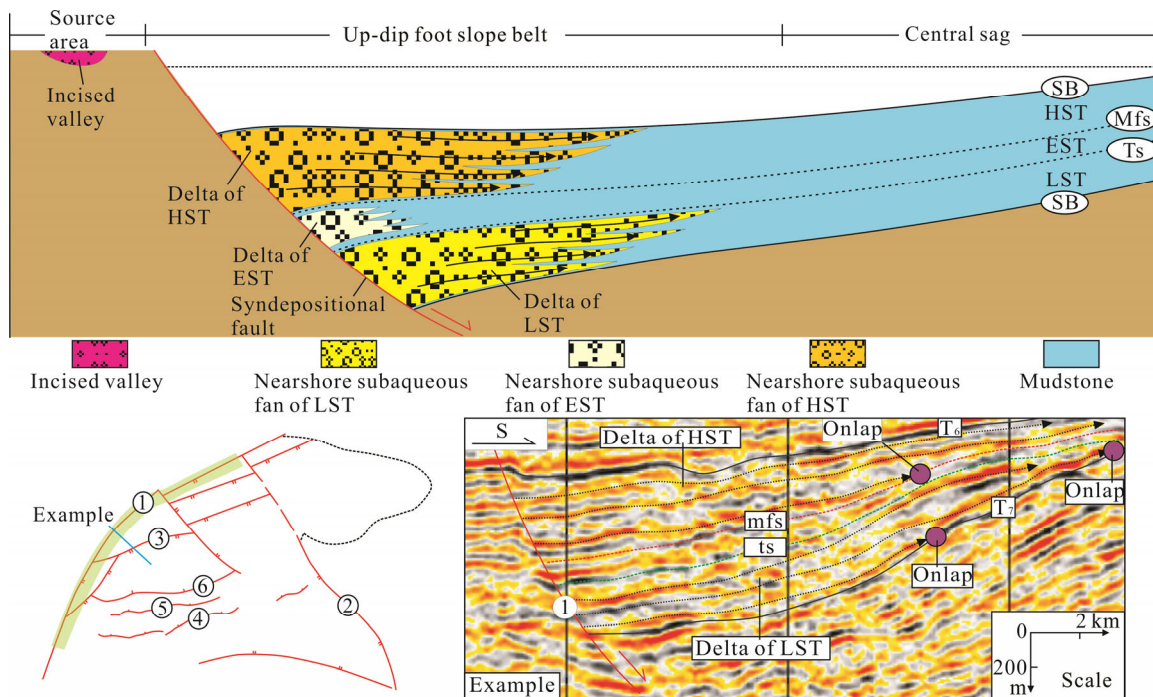


Figure 8. Up-dip foot slope belt and relevant sequence stratigraphic pattern (Type A1 Sequence). SB. Sequence boundary; HST. highstand system tracts; EST. expanding system tracts; LST. lowstand system tracts; ts. transgressive surface; mfs. maximum flooding surface.

which is the typical characteristic of slump fans. Due to the limited accommodation space resulted from the weak activity of Changliu fault, clasts can be transported to a farther distance. The thickness of Type A2 Sequence was much thinner and the areal extension of fans was much larger in comparison with Type A1 Sequence (Fig. 9).

5.2 Simple Gentle Slope and Relevant Sequence Stratigraphic Pattern

During the rifting stage I and initial rifting stage II, when Changliu Formation and the third member of Liushagang Formation were deposited, the simple gentle slope was developed along the southern ramp margin. Its relevant sequence stratigraphic pattern was named as Type B Sequence. Receiving clasts from the Hainan uplift, the Type B Sequence was mainly constituted by braided river deltas of lowstand and highstand system tracks. Core Wd (2 872.1 m), Core We (2 745.5 m), and Core Wf (2 732.7 m) show that the sediments change from poorly sorted mid-fine sandstones, through well sorted fine sandstones, siltstones to black mudstones in the lake centre. Braided deltas show medium-amplitude high-continuity seismic reflections with foreset geometry. Due to the uniform gradient and subdued topography, incised valleys, basin floor fans

or slope fans were absent during the lowstand system, and sedimentary strata thicken uniformly (Fig. 10).

5.3 Steep Slope Step-fault Belt and Relevant Sequence Stratigraphic Patterns

The steep slope step-fault belt, located in the northern escarpment margin, was characterized by two or three fault terraces that were jointly controlled by synsedimentary faults paralleling or sub-parallel to each other (Huang et al., 2012). As shown in Fig. 1, taking the Wushi fault as the boundary, the steep slope step-fault belt had two fault terraces jointly controlled by the Lingao fault and Chaoyang fault or Maniao fault in the west, but had three fault terraces jointly controlled by the Lingao fault, Beibu fault and Jinhe fault in the east. According to the differences in foot slope, steep slope step-fault belt can be further divided into two types: up-dip foot step-fault belt and down-dip foot step-fault belt.

5.3.1 Up-dip foot step-fault belt and relevant sequence stratigraphic pattern

The up-dip foot step-fault belt was developed at the middle-late rifting stage II, when the second and first members of the Liushagang Formation were deposited. We name the relevant

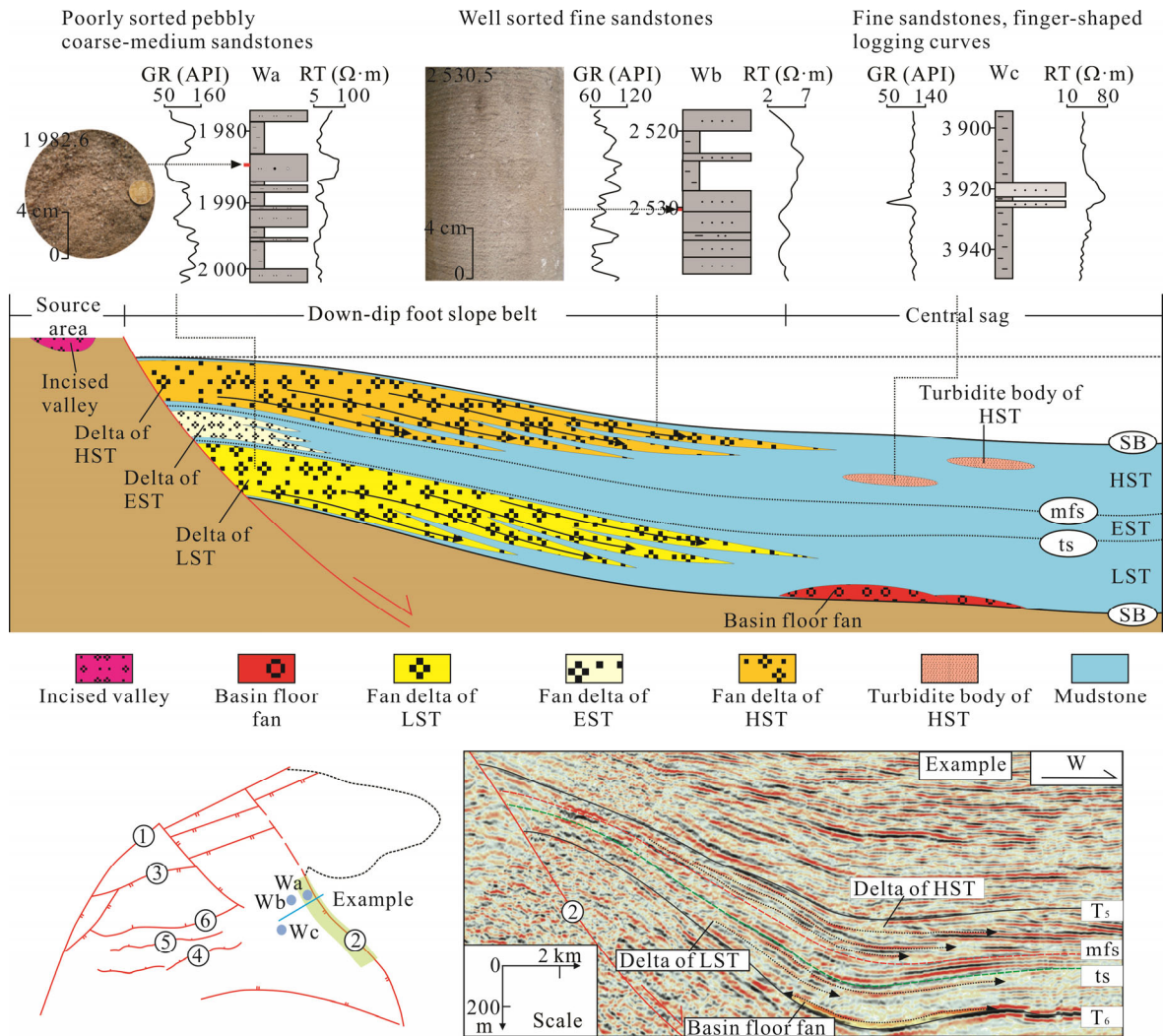


Figure 9. Down-dip foot slope belt and relevant sequence stratigraphic pattern (Type A2 Sequence).

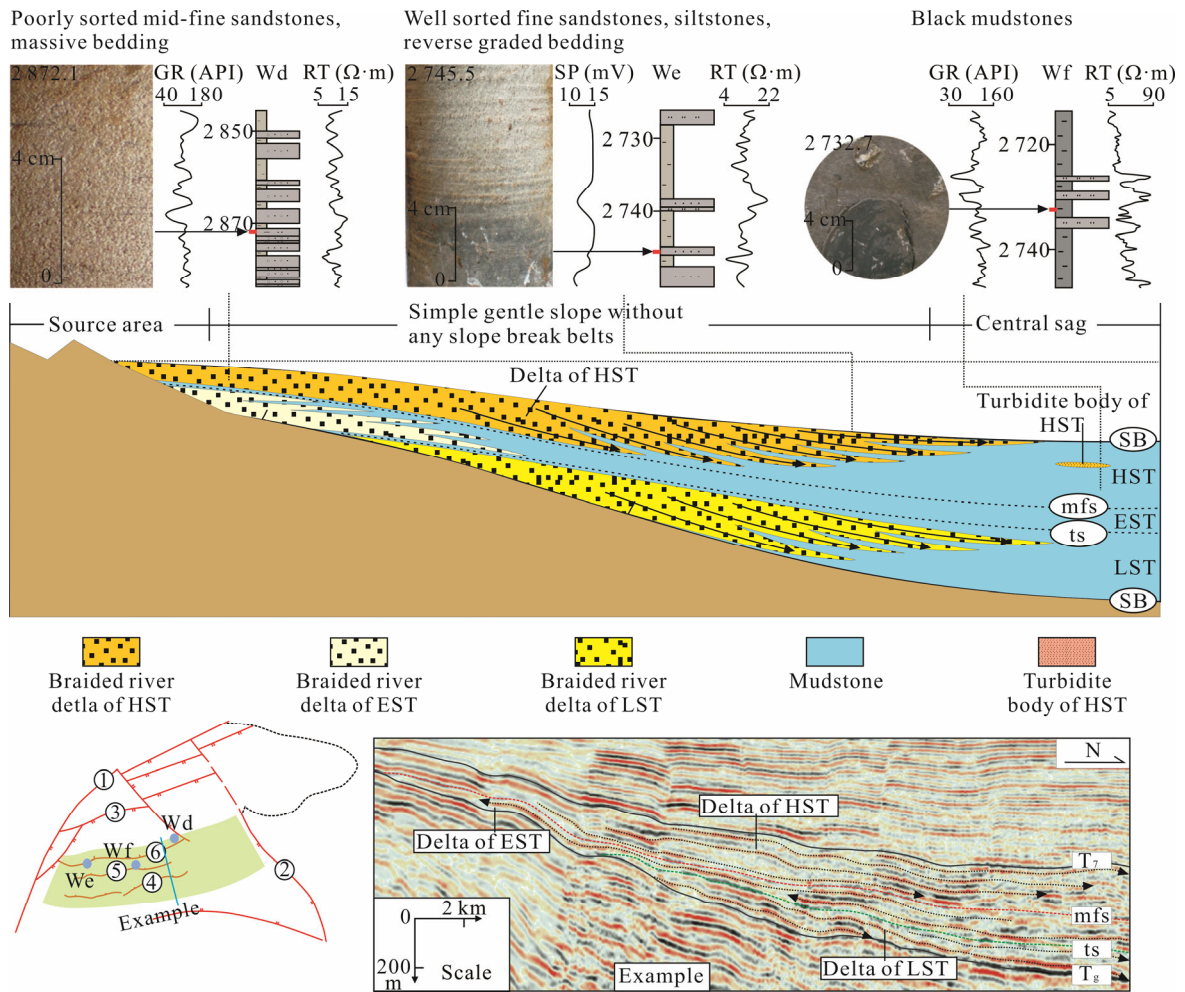


Figure 10. Simple gentle slope without any slope break belts and relevant sequence stratigraphic pattern (Type B Sequence).

sequence stratigraphic pattern as Type C1 Sequence. Take the up-dip foot step-fault belt developing along the west area of the northern escarpment margin for example to account the interval makeup of the Type C1 Sequence.

During the lowstand period, the base level fell below the Maniao fault. Underlying strata on the first fault terrace were exposed and eroded, with incised valleys forming. The sediments of Core Wg (3 127.2 m) are characterized by coarse-medium grained sandstones, and their log curves show zigzag box-shaped. These are typical characteristics of incised valley fillings. Clasts from the Lingao uplift were deposited on the second fault-terrace and formed nearshore subaqueous fans. Subsequently, the base level rose during the expanding and highstand periods. The Lingao fault formed the division between denuded and deposition zones. Nearshore subaqueous fans mainly developed on the downthrown wall of both the Lingao fault and Maniao fault. They show high-amplitude low-continuity reflection configurations on the seismic section. The lithology of fantails is mainly interbeds of medium-fine grained sandstone and mudstone, shown as Wg (2 529.6 m). Similar to Type A1 Sequence, slump fans of delta fronts were absent from the Type C1 Sequence (Fig. 11).

5.3.2 Down-dip foot step-fault belt and relevant sequence stratigraphic pattern

The down-dip foot step-fault belt was developed at the

rifting stage III, when the Weizhou Formation was deposited. We name the relevant sequence stratigraphic pattern as Type C2 Sequence. Take the down-dip foot step-fault belt developing along the west area of the northern escarpment margin for example to account the interval makeup of Type C2 Sequence.

During the lowstand period, the Maniao fault controlled the depositional boundary. Underlying strata on the first fault terrace were eroded, with incised valleys forming. Clasts were deposited on the second fault terrace and formed fan deltas. Subsequently, the base level rose during the expanding and highstand periods. The Lingao fault formed the division between denuded and deposition zones. The Maniao fault controlled a rapid thickening of sequence (Fig. 12). Fan-delta depositional systems were deposited on the first and second fault-terrace. Fan-delta fronts show medium-amplitude medium-continuity foreset reflection configurations on the seismic profile. Their main lithology is sandy conglomerates, pebbly fine sandstones, argillaceous siltstones, shown as Wi (2 750–2 790 m). Their log curve shows an obvious coarsening-upwards trend. Similar to Type A2 Sequence, basin floor fans and slope fans in the lowstand system tract (LST) and slump fans of delta fronts in the highstand system tract (HST) can directly deposited within the deep lake mudstones. Basin floor fans show a clear bidirectional downlap structure on the seismic profile. Core Wh (2 397.5 m) contains deformation structures and muddy debris, which are typical characteristics

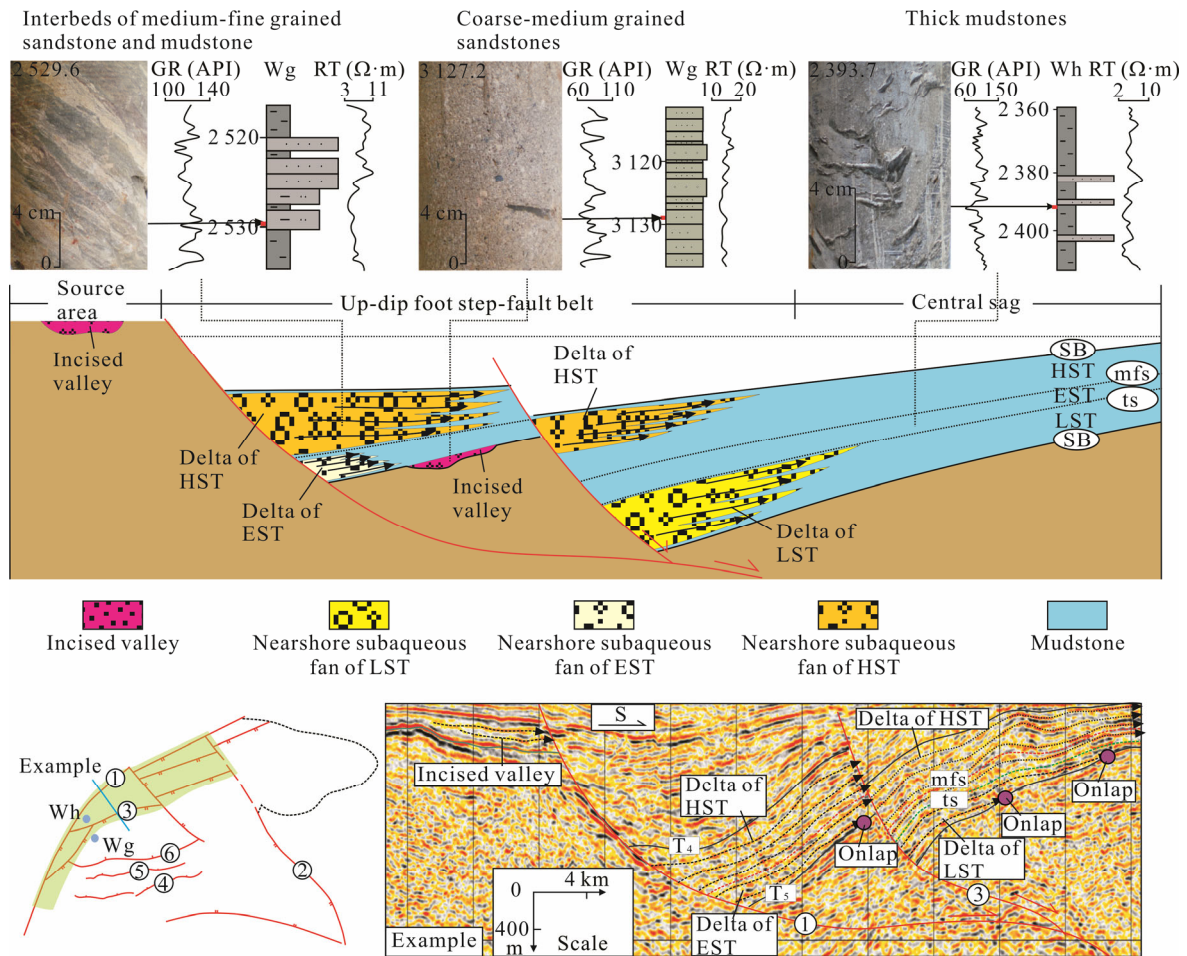


Figure 11. Up-dip foot step-fault belt and relevant sequence stratigraphic pattern (Type C1 Sequence).

of slump fans. As the fault activity became weaker and the subsidence rate became lower, shallower lake basin and limited accommodation space resulted in thinner Type C2 Sequence, but the areal extension of fan deltas was larger in comparison with Type C1 Sequence.

5.4 Multi-Level Step-Fault Belt and Relevant Sequence Stratigraphic Pattern

Multi-level step-fault belt was characterized by a multi-level fault terraces that were generated by a number of syndimentary faults along the ramp margin (Huang et al., 2012). In the Fushan sag, the multi-level step-fault belt was developed in middle-late rifting stage II and rifting stage III, along the west area of the southern ramp margin. We name the relevant sequence stratigraphic pattern as Type D Sequence.

During the lowstand period, the base level declined below the first fault. Receiving clasts from the Hainan uplift, sand bodies of braided delta fronts were mainly distributed on the second fault-terrace. Shown as Core Wj (2 827.9 m), the sediments of prodeltas are characterized by interbeds of sandstone and mudstone. Their log curve shows a coarsening-upwards trend. Basin floor fans were deposited on the third fault-terrace, forming lentiform sand bodies (Liu et al., 2014). The figer-shaped logging curve shown on Core Wk (3 120–3 150 m) is typical characteristic of basin floor fans. River plain channels were mainly developed above the first fault and formed incised

valleys. Core Wj (2 385.3 m) shows well sorted basal conglomerates of incised valley fillings. As the base level rose, the entire facies was drawn back. During the highstand period, the base level rose above the first fault. Because of abundant clast supply, sand bodies of braided river delta fronts can advance farther to the third fault-terrace. Slump fans of delta fronts were deposited directly within deep lake mudstones (Fig. 13). Therefore, with regular changes of lake level, various sedimentary facies of different periods were accumulated regularly on different fault-terraces from the sag edge to the center.

5.5 Slope Break Flexure Belt and Relevant Sequence Stratigraphic Pattern

The slope break flexure belt was developed in middle-late rifting stage II and rifting stage III, along the east area of the southern ramp margin. The relevant sequence stratigraphic pattern is named as Type E Sequence, which had characteristics similar to a typical Type I Sequence developed on passive continental margin (Ren et al., 2004). During the lowstand period, the base level declined below the slope break. Underlying strata above slope break were exposed and denuded, forming an unconformity surface. The basin floor fans and slope fans formed lenticular sand bodies in the deep lake (Liu et al., 2014). Subsequently, the base level rose during the expanding and highstand periods. The entire facies was drawn back. Across the slope break, the sequence thickness and the layer numbers

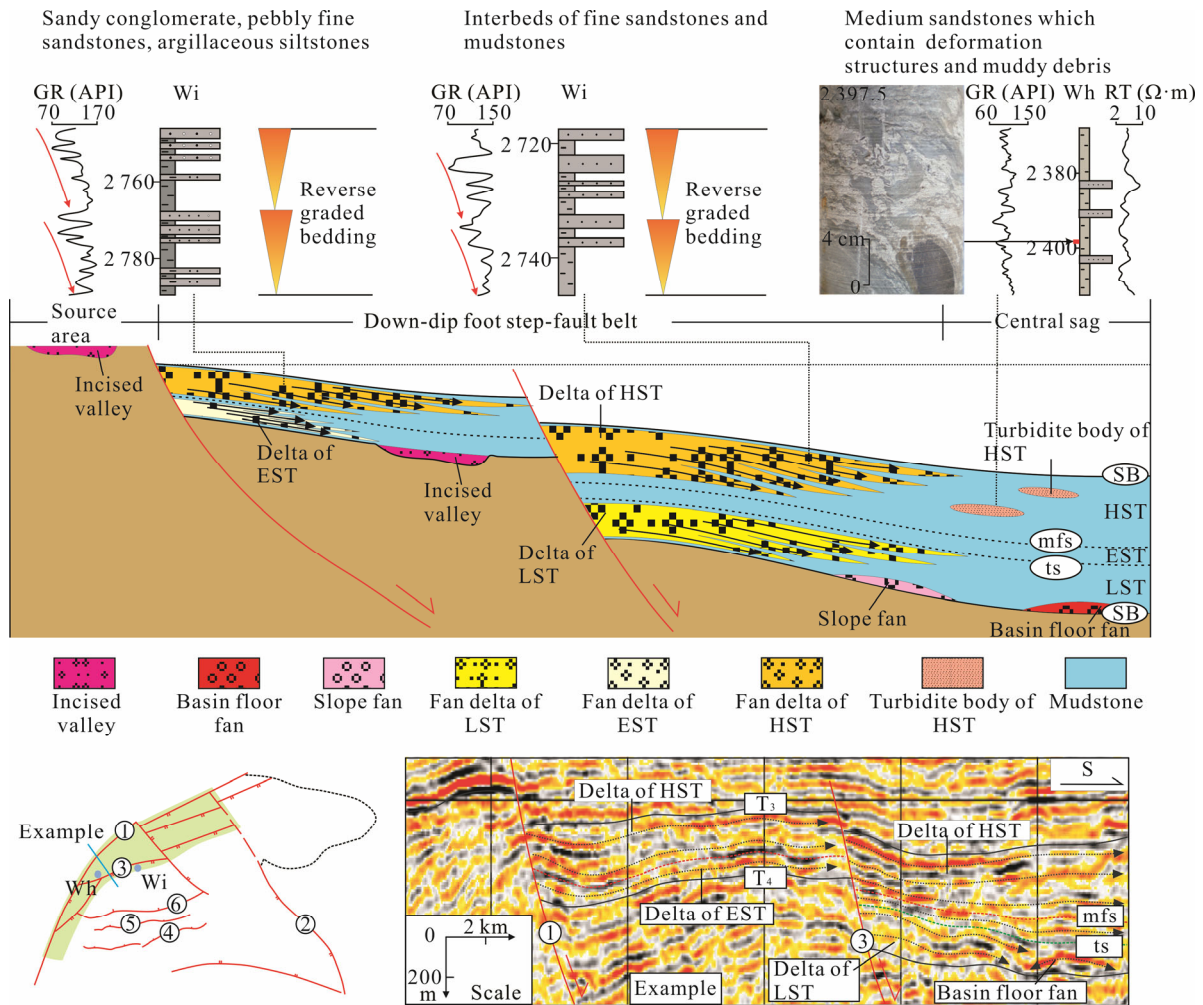


Figure 12. Down-dip foot step-fault belt and relevant sequence stratigraphic pattern (Type C2 Sequence).

and single layer thickness of sand bodies increased rapidly. Below the slope break, clear progradational reflection configurations can be shown on the seismic profile. Slump fans of delta fronts were directly deposited within the deep lake mudstones (Fig. 14). Core Wm (3 118.5 m) shows grey fine sandstones containing muddy bands, which is the characteristic of slump fans.

6 PALEOGENE TECTONIC EVOLUTION CONTROLS ON SEQUENCE STRATIGRAPHIC PATTERN

Based on all the above, the Paleogene tectonic evolution controls on the sequence stratigraphic patterns through controlling the structural slope break belts have been discussed as follows (Fig. 15).

(1) At the rifting stage I and initial rifting stage II, though the tectonic activity was not so intense, fault controlling action was the dominant mechanism. During this stage, the Fushan sag was characterized by simple “dustpan” shape dominated by the Lingao fault, which controlled subsidence centers along the northern escarpment margin. The growth rate of accommodation space generated by the activity of Lingao fault was greater than sedimentary accumulation rate. Therefore, the Type A1 Sequence dominated by up-dip foot slope belt was developed along the northern escarpment margin. However, the Changliu

fault, which had both extension and strike-slip characteristics, did not have so strong activity as the Lingao fault. The subsidence center was far away from the root of the Changliu fault. The growth rate of accommodation space generated by the activity of Changliu fault was smaller than sedimentary accumulation rate. Therefore, the Type A2 Sequence dominated by down-dip foot slope belt was developed along the eastern escarpment margin. Meanwhile, along the ramp margin, the paleogeomorphology was characterized by a simple gentle slope without any slope breaks, because the tectonic activity was not intense and its partition between the west and east was not obvious. Accordingly, the Type B Sequence was developed along the ramp margin.

(2) At the middle-late rifting stage II, as the tectonic activity strengthened, the paleogeomorphology of Fushan sag became complicated. Along the northern escarpment margin, the displacement of Lingao fault became so large that several concordant adjusting faults were formed. These faults were parallel or sub-parallel to the Lingao fault and presented a ladder-like profile. Fault controlling action was still the dominant mechanism. Subsidence centers were along the fault roots of Lingao fault and its adjusting faults. Abundant accumulation space generated by the activity of Lingao fault and its adjusting faults made the clasts deposit near fault roots. Therefore, the up-dip

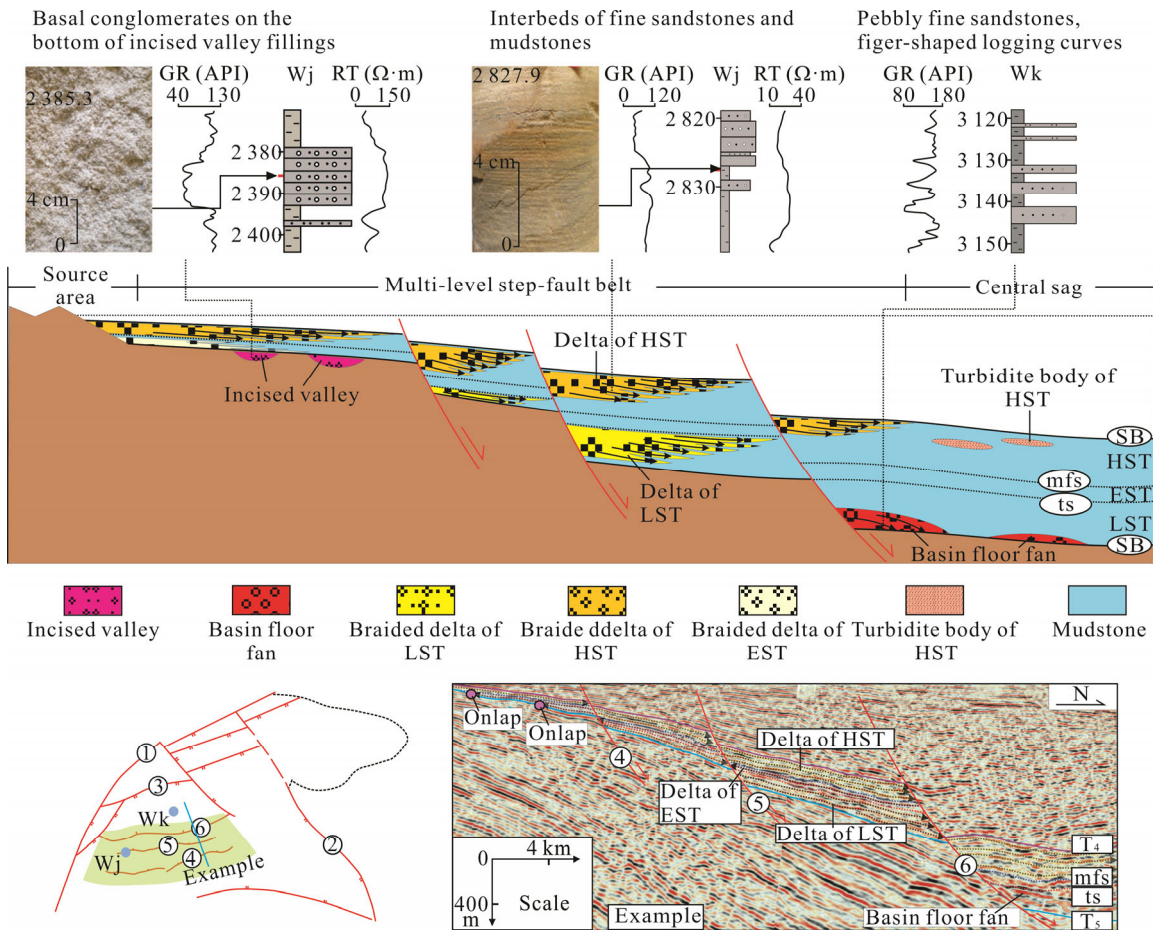


Figure 13. Multi-level step-fault belt and relevant sequence stratigraphic pattern (Type D Sequence).

foot step-fault belt and its relevant Type C1 Sequence were developed.

As the activity of Lingao fault strengthened, the topography of the ramp margin became steeper and steeper. Along the ramp margin, partition of the east and west in tectonic activity was particularly pronounced, resulting in different paleogeomorphology patterns between the east and west area. A number of NEE-extending adjusting faults parallel or sub-parallel to each other were developed along the west area of the ramp margin. These syndepositional faults presented a ladder-like profile, and formed multi-level step-fault belt. However, along the east area of the ramp margin, though the topography became steeper and steeper as a response to the enhanced activity of Lingao fault, weaker tectonic activity and smaller subsidence rate lead to gentler terrance in comparison with the west area. As a result, little syndepositional faults formed. The dispersion of depositional system along the east area of the ramp margin was mainly controlled by a slope break flexure belt, which was suggested to be caused by buried faults (Ma et al., 2012). In conclusion, during middle-late rifting stage II, Type D Sequence controlled by the multi-level step-fault belt was developed along the west area of the ramp margin, while Type E Sequence controlled by slope break flexure belt was developed along the east area.

During this period, the eastern escarpment margin was still dominated by down-dip foot slope belt and Type A2 Sequence.

(3) At the rifting stage III, as the tectonic activity weakened,

faults controlling action had been replaced by interaction of both territorial downwarp action and fault controlling action. Subsidence centers migrated from fault roots to sag center gradually. The growth rate of accommodation space generated by the activities of the Lingao fault and its adjusting faults was smaller than sedimentary accumulation rate. Therefore, the Type C2 Sequence controlled by down-dip foot step-fault belt was developed along the northern escarpment margin.

Meanwhile, the Type A2 Sequence, Type D Sequence and Type E Sequence continued to develop. However, their strata thickness became thinner and the areal extension of fans became larger, because weaker tectonic activity and smaller subsidence rate resulted in shallower lake basin, flatter topography and limited accommodation space.

In the Fushan sag, vertical evolution of structural slope break belts and relevant sequence stratigraphic patterns in Paleogene were strongly controlled by sag margin types and spatial differences in tectonic activity. The northern escarpment margin was controlled by the Lingao fault, which was characterized by the strongest activity among all the faults in Fushan sag (Fig. 6). Three evolution types of structural slope break belts indicate that the response of northern escarpment margin to Paleogene tectonic evolution was the most prominent. In contrast, the eastern escarpment margin was controlled by the Changliu fault, which featured weak activity (Fig. 6). One evolution type of structural slope break belts indicates that the eastern escarpment margin showed insignificant response to the Paleogene tectonic

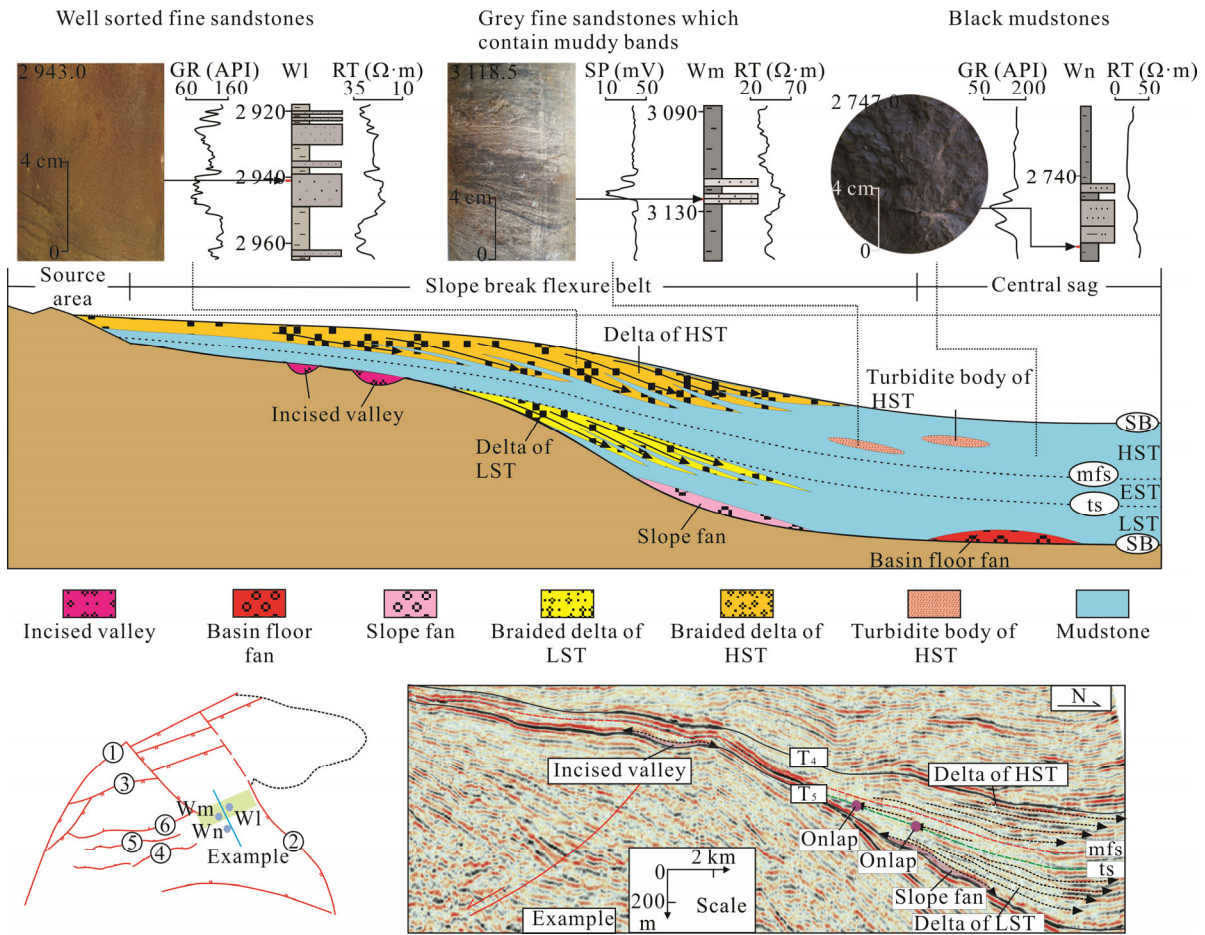


Figure 14. Slope break flexure belt and relevant sequence stratigraphic pattern (Type E Sequence).

Stratigraphy				Sequence stratigraphic pattern				Tectonic evolution			
System	Series	Formation	Member	Age (Ma)	Sequence boundary	Escarment margin		Ramp margin		Subsidence rate (m/Ma)	Rifting stage
						Northern escarpment margin	Eastern escarpment margin	West area	East area		
Paleogene	Oligocene	Weizhou	1	23.5	SB2					120-240	Rifting stage III
			2		SB21						
			3	30.0	SB3	Type C2 sequence	Type A2 sequence	Type D sequence	Type E sequence		
	Eocene	Liushagang	1	36.0	SB4	↑	↑	↑	↑	Tectonic subsidence rate Total subsidence rate	Rifting stage II
			2	40.0	SB5						
			3	44.0	SB6	Type C1 sequence	Type A2 sequence	Type D sequence	Type E sequence		
Paleocene	Changliu		49.0	SB7	↑	↑	↑	↑	Rifting stage I		
		65.0	SB8	Type A1 sequence	Type A2 sequence	Type B sequence	Type B sequence				

Figure 15. The control of tectonic evolution on sequence stratigraphic patterns.

evolution. Along the southern ramp margin, though both of the east and west areas manifested relatively prominent response to the Paleogene tectonic evolution, partition of the east and west in tectonic activity, especially during rifting stage II, leads to different evolution ways. According to the above discussion, four vertical evolution ways of structural slope break belts and relevant sequence stratigraphic patterns as a response to the Paleogene tectonic evolution can be concluded (Fig. 15). (1) “Up-dip foot slope belt—up-dip foot step-fault belt—down-dip foot step-fault belt” and its relevant “Type A1 Sequence—Type C1 Sequence—Type C2 Sequence” along the northern escarpment margin. (2) “Down-dip foot slope belt” and its relevant “Type A2 Sequence” along the eastern escarpment margin. (3) “Simple gentle slope without any slope breaks—multi-level step-fault belt” and its relevant “Type B Sequence—Type D Sequence” along the west area of the ramp margin. (4) “Simple gentle slope without any slope breaks—slope break flexure belt” and its relevant “Type B Sequence—Type E Sequence” along the east area of the ramp margin.

7 CONCLUSIONS

(1) The Paleogene system of the Fushan sag, northern South China Sea can be divided into one first-order sequence, three second-order sequences and seven third-order sequences on the basis of seismic data, complemented by drilling cores and well logs data.

(2) In the Fushan sag, through the analysis of paleotectonic stress field, unconformities and subsidence history, three tectonic episodes can be recognized in Paleogene: rifting stage I (65–49 Ma), rifting stage II (49–36 Ma), rifting stage III (36–23.5 Ma). Partition of the west and east in tectonic activity was obvious. The west area showed relatively stronger tectonic activity than the east area, especially during the rifting stage II.

(3) In the Fushan sag, four types of structural slope break belts were recognized: steep slope fault belt, steep slope step-fault belt, multi-level step-fault belt, slope break flexure belt. The first two can be further characterized as up-dip foot and down-dip foot. Multi-stage tectonic activities built a wide variety of structural slope break belts and further controlled different sequence stratigraphic patterns.

(4) In the Fushan sag, vertical evolution of structural slope break belts and relevant sequence stratigraphic patterns as a response to the Paleogene tectonic evolution was strongly controlled by sag margin types and spatial difference of tectonic activity. Four vertical evolution ways have been concluded, which not only enhances the understanding of tectonic evolution controls on sequence stratigraphic patterns, but also provides scientific evidence for predicting favorable exploration zones in particular tectonic positions under sequence stratigraphic framework.

ACKNOWLEDGMENTS

This study was supported by the National Natural Science Foundation of China (Nos. 41272122, 41202074). This paper benefited from 3D and 2D seismic data, drilling cores and well logs data provided by the South Oil Exploration and Development Company of PetroChina. The authors also express their appreciation for help provided by colleagues of South Oil Exploration and Development Company of Petro-

China. The final publication is available at Springer via <http://dx.doi.org/10.1007/s12583-015-0645-5>.

REFERENCES CITED

- Allen, P. A., Allen, J. R., 2005. Basin Analysis: Principle and Applications. Blackwell, Oxford. 1–493
- Catuneanu, O., Abreu, V., Bhattacharya, J. P., et al., 2009. Towards the Standardization of Sequence Stratigraphy. *Earth-Science Reviews*, 92(1/2): 1–33. doi:10.1016/j.earscirev.2008.10.003
- Deng, H. W., Guo, J. Y., Wang, R. J., et al., 2008. Tectono-Sequence Stratigraphic Analysis in Continental Faulted Basins. *Earth Science Frontier*, 15(2): 1–7 (in Chinese with English Abstract)
- Feng, Y. L., Xu, X. S., 2006. Syndepositional Structural Slope-Break Zone Controls on Lithologic Reservoirs—A Case from Paleogene Bohai Bay Basin. *Petroleum Exploration and Development*, 33(1): 22–31 (in Chinese with English Abstract)
- Feng, Y. L., Zhou, H. M., Ren, J. Y., et al., 2010. Paleogene Sequence Stratigraphy in the East of the Bohai Bay Basin and Its Response to Structural Movement. *Sci. Sin. Terrae*, 40(10): 1356–1376 (in Chinese with English Abstract)
- Haq, B. U., Hardenbol, J., Vail, P. R., 1987. Chronology of Fluctuating Sea Levels since the Triassic. *Science*, 235(4793): 1156–1167. doi:10.1126/science.235.4793.1156
- Huang, C. Y., Wang, H., Wu, Y. P., et al., 2012. Genetic Types and Sequence Stratigraphy Models of Palaeogene Slope Break Belts in Qikou Sag, Huanghua Depression, Bohai Bay Basin, Eastern China. *Sedimentary Geology*, 261/262: 65–75. doi:10.1016/j.sedgeo.2012.03.005
- Hou, Y. G., He, S., Ni, J. E., et al., 2012. Tectono-Sequence Stratigraphic Analysis on Paleogene Shahejie Formation in the Banqiao Sub-Basin, Eastern China. *Marine and Petroleum Geology*, 36(1): 100–117. doi:10.1016/j.marpetgeo.2012.06.001
- Lei, C., Ren, J. Y., Li, X. S., et al., 2011. Structural Characteristics and Petroleum Exploration Potential in the Deep-Water Area of the Qiongdongnan Basin, South China Sea. *Petroleum Exploration and Development*, 38(5): 560–569 (in Chinese with English Abstract)
- Li, S. T., Lin, C. S., Zhang, Q. M., et al., 1999. Episodic Rifting of Continental Marginal Basins and Tectonic Events since 10 Ma in the South China Sea. *Chinese Science Bulletin*, 44(1): 10–23. doi:10.1007/bf03182877
- Li, S. T., Pan, Y. L., Lu, Y. C., et al., 2002. Key Technology of Prospecting and Exploration of Subtle Traps in Lacustrine Fault Basins: Sequence Stratigraphic Researches on the Basis of High Resolution Seismic Survey. *Earth Science—Journal of China University of Geosciences*, 27: 592–598 (in Chinese with English Abstract)
- Li, S. T., Xie, X. N., Wang, H., et al., 2004. Sedimentary Basin Analysis Principle and Application. Higher Education Press, Beijing. 1–410 (in Chinese)
- Liao, J. H., Wang, H., Sun, Z. P., et al., 2012. Tectonic Evolution and Its Controlling on Sequence Pattern of Chang-Chang Sag, Deepwater Area of Qiongdongnan Basin, South China Sea. *Journal of Central South University (Science and Technology)*, 43: 3121–3132 (in Chinese)

- with English Abstract)
- Lin, C. S., 2009. Sequence and Depositional Architecture of Sedimentary Basin and Process Responses. *Acta Sedimentologica Sinica*, 27: 849–862 (in Chinese with English Abstract)
- Lin, C. S., Kenneth, E., Li, S. T., et al., 2001. Sequence Architecture, Depositional Systems, and Controls on Development of Lacustrine Basin Fills in Part of the Earlian Basin, Northeast China. *AAPG Bulletin*, 85(11): 2017–2043
- Lin, C. S., Zhang, Y. M., Li, S. T., et al., 2004. Episodic Rifting Dynamic Process and Quantitative Model of Mesozoic–Cenozoic Faulted Basins in Eastern China. *Earth Science—Journal of China University of Geosciences*, 29(5): 583–588 (in Chinese with English Abstract)
- Liu, E. T., Wang, H., Lin, Z. L., et al., 2012. Characteristics and Hydrocarbon Enrichment Rules of Transfer Zone in Fushan Sag, Beibuwan Basin. *Journal of Central South University (Science and Technology)*, 43: 3946–3953 (in Chinese with English Abstract)
- Liu, E. T., Wang, H., Li, Y., et al., 2014. Sedimentary Characteristics and Tectonic Setting of Sublacustrine Fans in a Half-Graben Rift Depression, Beibuwan Basin, South China Sea. *Marine and Petroleum Geology*, 52: 9–21. doi:10.1016/j.marpetgeo.2014.01.008
- Liu, H., Wang, Y. M., Xin, R. C., et al., 2006. Study on the Slope Break Belts in the Jurassic Down-Warped Lacustrine Basin in Western-Margin Area, Junggar Basin, Northwestern China. *Marine and Petroleum Geology*, 23(9/10): 913–930. doi:10.1016/j.marpetgeo.2006.08.004
- Liu, L. J., Kuang, H. W., Tong, Y. M., et al., 2003. Sedimentary Systems and Evolution Characteristics of Lower Tertiary Liushagang Formation in Fushan Sag. *Oil & Gas Geology*, 24(2): 140–145 (in Chinese with English Abstract)
- Ma, Q. L., Zhao, S. E., Liao, Y. T., et al., 2012. Sequence Architectures of Paleogene Liushagang Formation and Its Significance in Fushan Sag of the Reibuwan Basin. *Earth Science—Journal of China University of Geosciences*, 37(4): 667–678 (in Chinese with English Abstract)
- Ma, Y., Li, S. Z., Zhang, B. K., et al., 2013. Unconformities in the Beibuwan Basin and Their Implications for Tectonic Evolution. *Marine Geology & Quaternary Geology*, 33(2): 63–72 (in Chinese with English Abstract)
- Ren, J. Y., Lu, Y. C., Zhang, Q. L., et al., 2004. Forming Mechanism of Structural Slope-Break and Its Control on Sequence Style in Faulted Basin. *Earth Science—Journal of China University of Geosciences*, 29(5): 596–602 (in Chinese with English Abstract)
- Shi, Y. M., Liu, J., Zhang, M. Z., et al., 2007. Experience and Understand in Oil and Gas Exploration in Fushan Sag, Hainan Province. *South China Journal of Selsmology*, 27(3): 57–68 (in Chinese with English Abstract)
- Song, G. Z., Wang, H., Gan, H. J., et al., 2014. Paleogene Tectonic Evolution Controls on Sequence Stratigraphic Patterns in the Central Part of Deepwater Area of Qiongdongnan Basin, Northern South China Sea. *Journal of Earth Science*, 25(2): 275–288. doi:10.1007/s12583-014-0433-7
- Van Wagoner, J. C., Mitchum, R. M., Campion, K., et al., 1990. Siliciclastic Sequence Stratigraphy in Well Logs, Cores and Outcrops: Concepts for High Resolution Correlation of Time and Facies. *AAPG Methods in Exploration Series*, 7: 1–55
- Vail, P. R., Mitchum, R. M., Thompson, S., 1977. Global Cycles of Relative Changes of Sea Level. *AAPG Bulletin*, 26: 99–116
- Wang, G. H., Huang, C. Y., Liu, E. T., et al., 2014. Characteristics of Slope-Breaks and Its Control on Sedimentation and Hydrocarbon Accumulation of Liushagang Formation in Gentle Slope, South Fushan Sag. *Journal of Central South University (Science and Technology)*, 45(5): 1–11 (in Chinese with English Abstract)
- Xie, X. N., Müller, R. D., Ren, J. Y., et al., 2008. Stratigraphic Architecture and Evolution of the Continental Slope System in Offshore Hainan, Northern South China Sea. *Marine Geology*, 247(3/4): 129–144. doi:10.1016/j.margeo.2007.08.005
- Xu, H., 1997. Some Problems in Study of Continental Sequence Stratigraphy. *Oil & Gas Geology*, 18: 83–89 (in Chinese with English Abstract)
- Xu, J. Y., Zhang, G. C., Liang, J. S., et al., 2011. Paleogene Activities of Episode Rifting and Their Relationships with Hydrocarbon in Beibuwan Basin. *China Offshore Oil and Gas*, 23(6): 362–368 (in Chinese with English Abstract)
- Zhang, Z. W., Liu, Z. F., Zhang, G. C., et al., 2013. The Chasmic Stage and Structural Evolution Features of Beibuwan Basin. *Journal of Oil and Gas Technology*, 35(1): 6–10 (in Chinese with English Abstract)